Available online at www.sciencedirect.com
SCIENCE DIRECT
Journal of Physics and Chemistry of Solids 66 (2005) 861–868
JOURNAL OF PHYSICS AND CHEMISTRY OF SOLIDS
www.elsevier.com/locate/jpcs

Investigation of Cu and Co multilayer deposition in aqueous ambient

Dhirendra Gupta, A.C. Nayak, D. Kaushik, R.K. Pandey*

Department of Physics, Bhopal University, Bhopal, MP 462026, India

Received 30 January 2004; accepted 9 November 2004

Abstract

Electrochemical preparation of multilayers of Cu/Co(Cu) has been investigated using cyclic voltammetry and in situ atomic force microscopy. Potentiostatic pulse deposition of Copper and Cobalt has been shown to reduce the surface roughness of the electrodeposits. Multilayers of Cu/Co(Cu) have been grown electrochemically using pulse deposition technique. Formation of coherent multilayers has been demonstrated using grazing angle X-ray diffraction studies.

Keywords: A. Multilayers

1. Introduction

The multilayers of copper and cobalt/nickel find application in high-density magnetic storage media, GMR sensors, hard coatings [1–4], etc. Physical evaporation techniques viz sputtering, molecular beam epitaxy (MBE), electron beam evaporation and pulse laser ablation [5–11] have been extensively used to grow multilayers of these elements. Recently multilayered nanowires of copper/cobalt and copper/nickel [12,13] have also been grown for possible application in microwave switching devices. Since this will require growth inside fine cavities, physical techniques are inherently unsuitable. Electrodeposition is expected to offer a cost effective alternative for such applications. Fabrication of complex three-dimensional structures can also be accomplished using electrodeposition technique. Recently, attempts have been made to electrodeposit alloys [14–17] and multilayer of the copper, nickel and/or cobalt [18–21]. These multilayers require sharp interfaces and highly smooth surfaces for large GMR. It is, therefore, necessary to investigate the electrochemical processes and the evolution of the surface morphology in situ during the electrodeposition. We have, therefore, carried out extensive systematic studies on these aspects for the electrodeposited Cu/Co multilayered films and the results have been presented in this paper.

2. Experimental details

All the electrochemical investigations were carried out inside a glass cell using a three electrode geometry. The counter electrode was made from high purity platinum foil. An ITO coated glass substrate served as the working electrode whose potential was monitored with respect to a saturated calomel electrode, connected to the electrochemical cell through a luggin capillary. All the electrodes were kept in position with the help of a teflon screw thread joint. The electrochemical cell had inlet and outlet ports through which fresh electrolyte was continuously replenished. All cyclic voltammetry experiments reported in this work were performed using a scan rate of 2 mV/s.

Multilayers were prepared using the standard bath containing. $CoSO_4 \cdot 6H_2O$ (0.5 M), $NiSO_4 \cdot 5H_2O$(0.1 M), $NiCl_2$ (0.02 M), Boric Acid (0.45 M) and $CuSO_4 \cdot 5H_2O$ (0.004 M) in triple distilled water at pH 1.9−2.1. A cold rolled copper foil polished to a 0.1 μm finish, was used as a substrate for multilayer growth. The typical pulse voltage and pulse current employed for the deposition have been shown in Fig. 1(a) and (b). The typical

* Corresponding author. Tel.: +91 755 267 7723; fax: +91 755 26 777 22.
E-mail address: ipebu@sancharnet.in (R.K. Pandey).

0022-3697/$ - see front matter © 2004 Published by Elsevier Ltd.
doi:10.1016/j.jpcs.2004.11.007

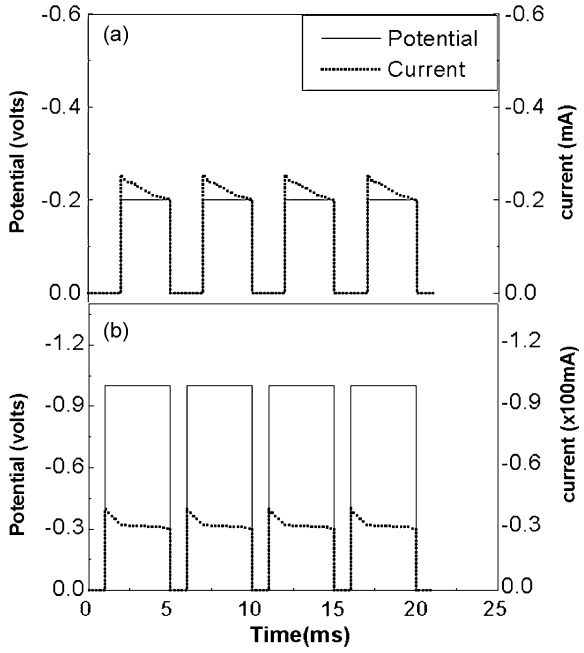

Fig. 1. A typical Pulse potential and corresponding current waveform used for (a) copper and (b) cobalt deposition, respectively.

frequencies and duty cycles employed for the electrodeposition of Cu and Co were 200 Hz, 60% and 400 Hz, 80%, respectively. The Cu and Co deposition programmes were alternatively triggered for 10 and 1 s, respectively. A delay time of 1 s was deliberately introduced between Co and Cu pulse to allow the interfacial concentrations to attain equilibrium.

The surface morphology of deposited layers were studied in situ in a specially designed miniaturised cell using a wet atomic force microscope (Shimadzu model SPM 9500J2). A 125μ×125 μm peizoscanner with a vertical z-axis resolution of 1 nm was employed for surface imaging with a scan rate of 2 Hz. Imaging was carried out using 20 nm wide legged silicon nitride cantilevers (spring constant 1.4−2.4 N/m) in contact mode. Before scanning, the condition of the cantilever was cross-examined by taking the images of a freshly cleaved mica surface. The electrodeposition was, initially allowed to proceed for a predetermined duration. Images of the surface were captured following the interruption of the electrodeposition programme to ensure that external applied electric field does not affect the cantilever motion.

Microstructure of the electrodeposited multilayers and bilayer period were investigated with the help of a Shimadzu, Japan X-ray diffractometer (XRD 6000). Glancing angle X-ray diffraction patterns (GAXRD) were also recorded between 2θ interval of 40–55° with glancing angle of 1°. A 0.05 mm divergence slit was employed to reduce the beam divergence. A graphite monochromator placed on the detector side was used to filter Cuk_{β} radiation. Data were recorded using continuous scan @ 1° per min.

3. Results and discussions

3.1. Cyclic voltammetry

It is possible to electrodeposit relatively pure copper films in presence of cobalt and nickel ions in the electrolyte due to the very positive standard reduction potential (−0.09 V vs SCE) for copper, as compared to nickel (−0.49 V) and cobalt (−0.52 V). However, nickel and cobalt exhibit anomalous codeposition behavior [22,23]. Consequently, nickel electrodeposition is inhibited in presence of cobalt. The electrochemical processes involved during the electrodeposition of these elements, in the standard bath were investigated using slow scan cyclic voltammetry. Fig. 2(a) shows a typical cyclic voltammogramme obtained by sweeping the ITO working electrode potential between +0.4 and −0.4 V using a scan rate of 2 mV/s. The rest potential of the ITO substrate in the bath was +0.24 volts. The first cathodic onset recorded at −0.15 V implied the onset for reduction of copper ions. Continuing the potential sweep to negative values yielded

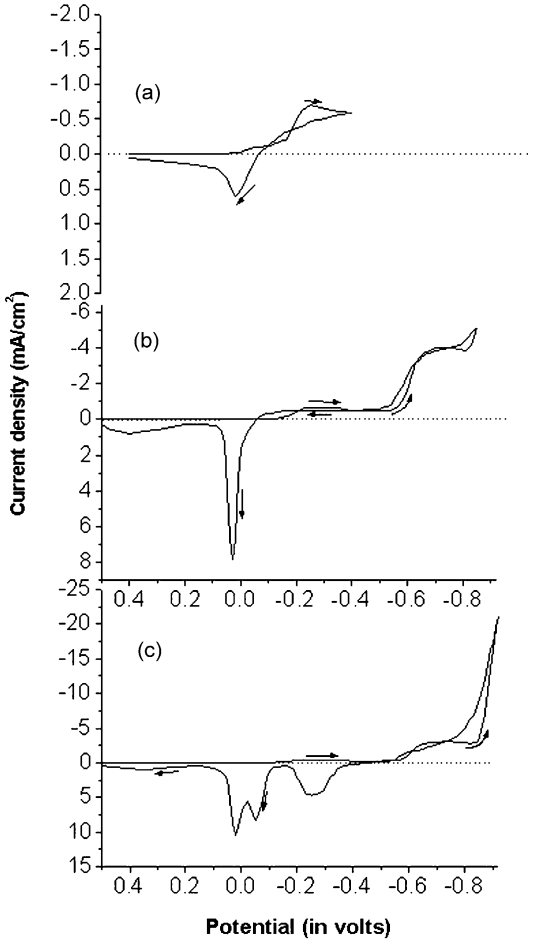

Fig. 2. Cyclic Voltammogrammes recorded in electrolytes containing 0.5 M $CoSO_4 \cdot 7H_2O$, 0.004 M $CuSO_4 \cdot 5H_2O$, 0.45 Boric acid 0.02 $NiCl_2 \cdot 5H_2O$ and 0.12 M, $NiSO_4 \cdot 6H_2O$ during scan between (a) +0.4 and −0.4 V (b) +0.4 and −0.85 V and (c) +0.4 and −0.92 V. Scan rate=2 mV/s.

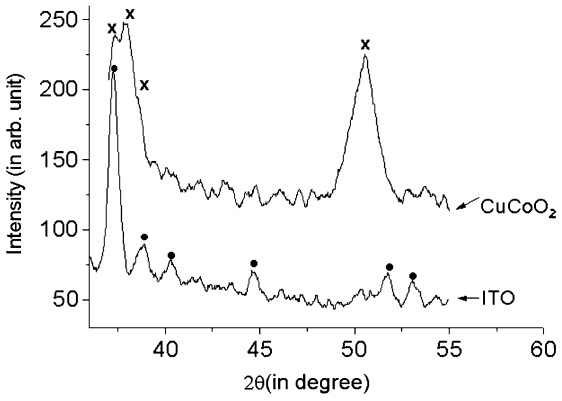

Fig. 3. X-ray diffraction data recorded for a film deposited on ITO-coated substrate at −0.65 V. The peaks marked as '×' corresponds to $CuCoO_2$ while the peaks marked as '●' corresponds to the ITO substrate.

a cathodic peak at −0.25 V. During the reverse sweep between −0.4 V and the crossover point the current always remained less than the corresponding cathodic current. The existence of a diffusion bottleneck to the kinetically controlled reduction of copper may give rise to such a behavior. The anodic peak at +0.02 V shown in the Fig. 2(a) corresponds to the deplating of electrodeposited copper. In another experiment, when the cathodic sweep was continued up to −0.85 V, two distinct features were recorded and shown in Fig. 2(b). A limiting current plateau between −0.25 and −0.57 V was attributed to the diffusion controlled deposition of copper. The corresponding limiting current density was 0.2 mA/cm^2. Interestingly, a second cathodic onset was observed at −0.57 V with a shoulder at −0.65 V. The second cathodic onset was recorded even in the absence of copper and nickel ions in the bath. These characteristic features were therefore, assigned to cobalt species.

In order to establish the identity of the deposit phase obtained at −0.65 V, structural characterization was carried out using grazing angle XRD with the angle of incident fixed at 0.5°. Fig. 3 shows the result of the grazing angle X-ray diffraction pattern exhibited by the electrodeposited film grown at −0.65 V on ITO substrate for 5 min. The diffraction pattern contributed by the substrate has also been shown in the figure (lower curve). The experimentally determined d-values matched with the corresponding JCPD data for $CoCuO_2$ as shown in Table 1. Note that the first peak observed at $2\theta = 37.30°$ is shared by the ITO base layer as well as the oxide film. It is therefore, difficult to uniquely assigns its origin to the deposited phase. The other three peaks marked as '×' recorded at $2\theta = 37.82°$, 38.60° and 50.40° were, however, contributed only by the electrodeposited oxide.

Table 1
Peak positions and d- values obtained from X-ray diffraction data of $CoCuO_2$ film

Sr. no.	Observed			Standard	
	2θ value (in degree)	d-value (Å)	I/I_1	d-value (Å)	I/I_1
1	37.30	2.41	51	2.42	20
2	37.82	2.37	72	2.38	50
3	38.60	2.33	28	2.35	100
4	50.40	1.81	100	1.86	30

It is, therefore, unambiguously concluded that the cathodic shoulder at −0.65 V can be assigned to the formation of $CoCuO_2$. The oxide formation in the aqueous bath occurs due to the interference of a concomitant oxygen reduction reaction along with that of copper and cobalt. Earlier, using Pourbaix diagram, Bahrololoom et al. [24] have suggested that cobalt can form different oxides/hydroxide even in acidic solutions. Further, Jiang et al. [25] have also suggested that oxide of cobalt may be formed during cathodic reduction in presence of oxygen.

The anodic back sweep shown in Fig. 2(b) resulted in two peaks at +0.03 and +0.4 V. The former peak was also observed by Jiang et al. [25] and was assigned to the formation of $Co(OH)_2$. The latter peak originates due to the anodic stripping of electrodeposited copper.

Fig. 2(c) shows the typical voltammogramme recorded when cathodic sweep was extended till −0.92 V. Sharp rise in the cathodic current beyond −0.83 V implied kinetically controlled reduction of cobalt. Due to the close proximity of the reduction potential for nickel, however, its electrocodeposition can not be ruled out. Deposition of bright metallic coatings of Co were indeed noticed beyond this potential. The anodic back sweep revealed four peaks at −0.25, −0.05, +0.02 and +0.35 V. While the most anodic peak (+0.35 V) recorded in our studies has its origin to copper stripping, the first two peaks may correspond to the formation of hydroxide and dissolution of cobalt.

The anodic peak recorded at − 0.02 V, was a new peak seen in presence of nickel ions only and hence can be attributed to Ni striping. In an earlier report [26], it has been shown that the presence of small concentration of nickel ions in the bath is helpful in retarding the cobalt dissolution process.

3.2. Compositional analysis

The composition of two typical films electrodeposited at −0.35 and −1.1 V, respectively, were analysed using atomic absorption spectroscopy (AAS). The results have been summarised in Table 2. As expected, the former film

Table 2
Composition of the Cu/Co film deposited at two different potentials as determined using atomic absorption spectroscopy

Film	Pulse potential (vs SCE) (V)	Film composition (%)		
		Cu	Co	Ni
1	−0.35	99.99	–	–
2	−1.1	4.37	95.63	Trace

predominantly contained copper. The presence of cobalt and nickel could not be detected in the film. This is in agreement with our expectation since at −0.35 V, only copper is expected to electrodeposit. The film electrodeposited at −1.1 V, were, however, found to contain predominantly cobalt (95.63%). A small concentration (4.37%) of copper was also detected in the film. It is, therefore, concluded that at this potential, both cobalt and copper deposit together though the latter is in small concentration. It is interesting to remark that our AAS analysis could not detect presence of nickel in the film. Nickel if present, might be in trace quantity only. The relative absence of nickel in the film could be attributed to the cumulative effect of the use of short electrodeposition pulse and the inhibition of electrodeposition of nickel in presence of cobalt.

3.3. AFM investigations

Fig. 4 represents the two−dimensional surface morphology alongwith roughness profile of polished copper substrate imaged in side the electrolyte prior to deposition. The deep ridges seen on the surface might have originated due to mechanical polishing. The average roughness of the surface was determined to be 2.75 nm. Conventional dc potentiostatic deposition is expected to amplify the surface roughness of the deposit as the electrodeposition proceeds. However, it can be shown [27] that this problem can be considerably mitigated with the help of a pulse deposition cycle. The pulse programme employed in the present electrodeposition experiments was expected to achieve this objective. To vindicate our assumption, in situ wet atomic force microscopy experiments were also undertaken to examine evolution of the surface morphology of successively electrodeposited layers. The substrate surface was continuously scanned following an electrodeposition pulse of known duration. Fig. 5(a)–(c) represent the two dimensional surface morphologies recorded following 2, 4.5 and 10 s of deposition of copper. In all these cases, the pulse duty cycle and repetition rate were always kept constant. The average current density was approximately 0.2 mA/cm^2. Note that the electrodeposition duration of 2 s leads to the formation of polycrystalline growth of copper. Growth of faceted grains of copper can be distinctly seen on the surface following 4.5 s of deposition in Fig. 5(b). Full surface coverage was seen following 10 s of electrodeposition of copper as shown in Fig. 5(c). In all the three cases the electrodeposited copper films were characterized by a nodular grain growth. The histograms showing the evolution of grain size with deposition duration of 2, 4.5, and10 s, respectively, have also been shown in Fig. 5 alongwith the corresponding surface morphologies. It is seen that the majority of grains following 2 s of deposition have size of approximately 50 nm ± 11%. However, few grains of size as small as 20 nm and as large as 80 nm were also seen. The large distribution in grain size observed in our studies is a typical feature of three-dimensional nucleation. As the electrodeposition was allowed to proceed for 4.5 sec, the grain size further increased. The majority of grains now possessed size of ∼130 nm, but the size distribution is now considerably reduced to ±7.6%. Allowing the electrodeposition to proceed for 10 s did not lead to any substantial enhancement in grain size (146 nm ± 7.5%) as shown in Fig. 5(c) by the corresponding histogram.

In situ measurements of surface roughness were also carried out using atomic force microscopy. For this purpose different area of the substrate were repeatedly scanned and each of the area was analyzed in different directions for surface roughness calculations. The average surface roughness of copper film following 2 and 4.5 s of deposition were 1.8 and 1.3 nm, respectively. Note that the surface roughness of the electrodeposited copper is much smaller then the measured surface roughness of the substrate. Our results clearly vindicate the assumption that pulse deposition can considerably reduce the surface roughness of the electrodeposit.

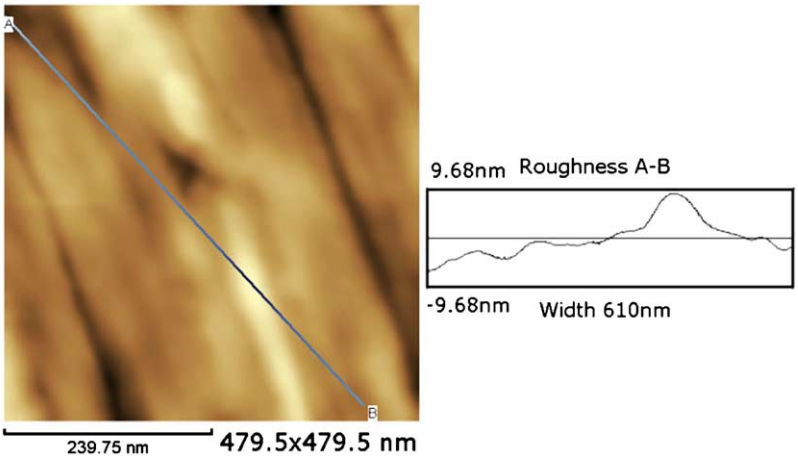

Fig. 4. Two dimensional AFM image and roughness profile of a polished copper substrate.

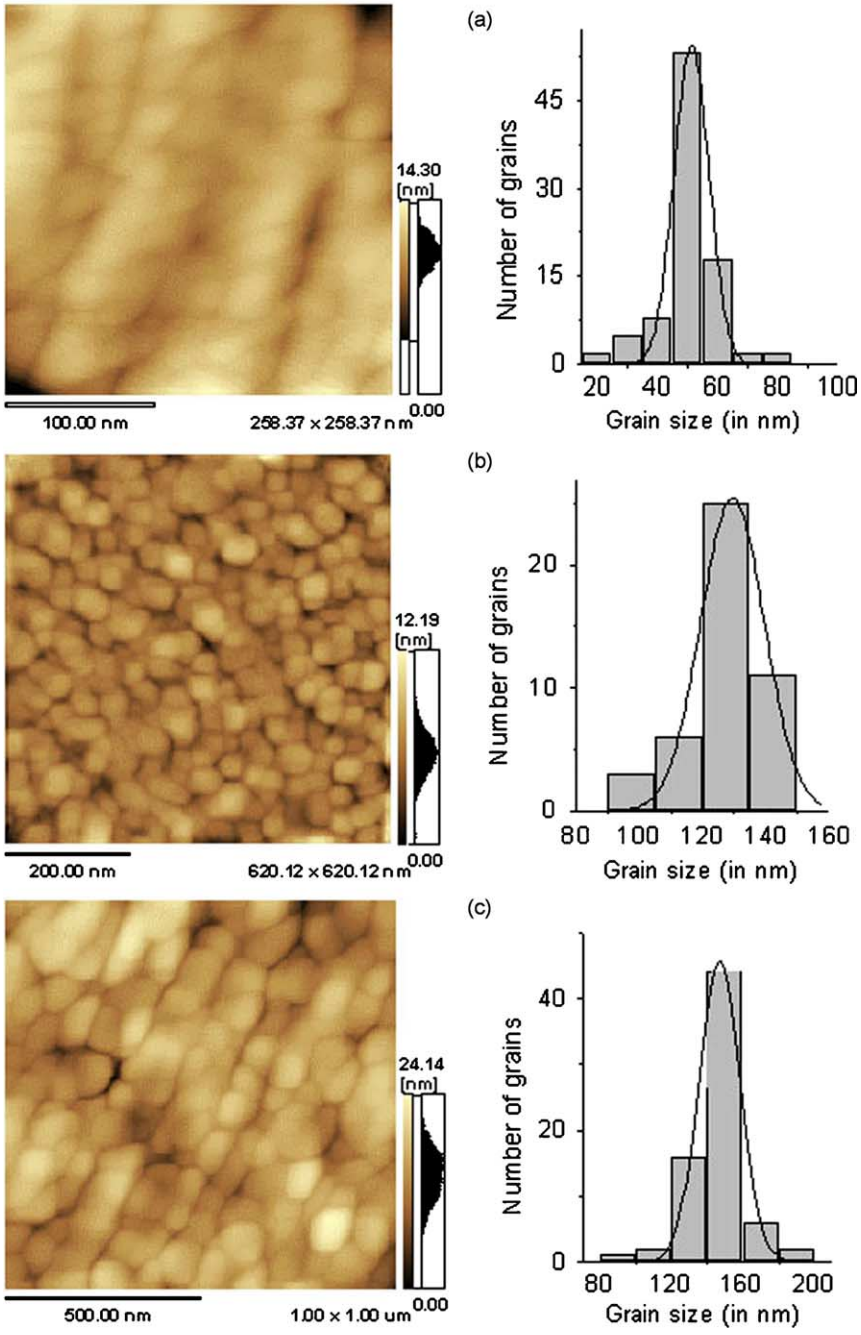

Fig. 5. Typical two dimensional AFM images of copper films deposited for (a) 2 (b) 4.5 and (c) 10 s along with the corresponding histograms showing grain size distribution.

In situ examination of the morphology of the electrodeposited cobalt film was also carried out and the results are shown in Fig. 6(a) and (b) following 1 and 3 s of electrodeposition, respectively. For both the cases, growth of a compact granular polycrystalline film can be seen. The average surface roughness for all these films was 1.1 nm.

The Gaussian fit of the histograms of grain size variation for the electrodeposited cobalt film after 1 and 3 s of deposition have been shown on the right side of Fig. 6(a) and (b). The mean grain size for the former film was calculated as 52 nm $\pm$ 15%, while for the later film it was 43 nm $\pm$ 20%. Obviously the grain size of the cobalt film did not change significantly for longer deposition duration.

Finally, AFM image of the top surface (Co) was also recorded following deposition of 40 bilayer periods of Cu and Co(Cu) and the result has been shown in Fig. 7. The average surface roughness of this film was found to be 1.3 nm, respectively. From our in situ AFM studies it can thus be concluded that the surface roughness of

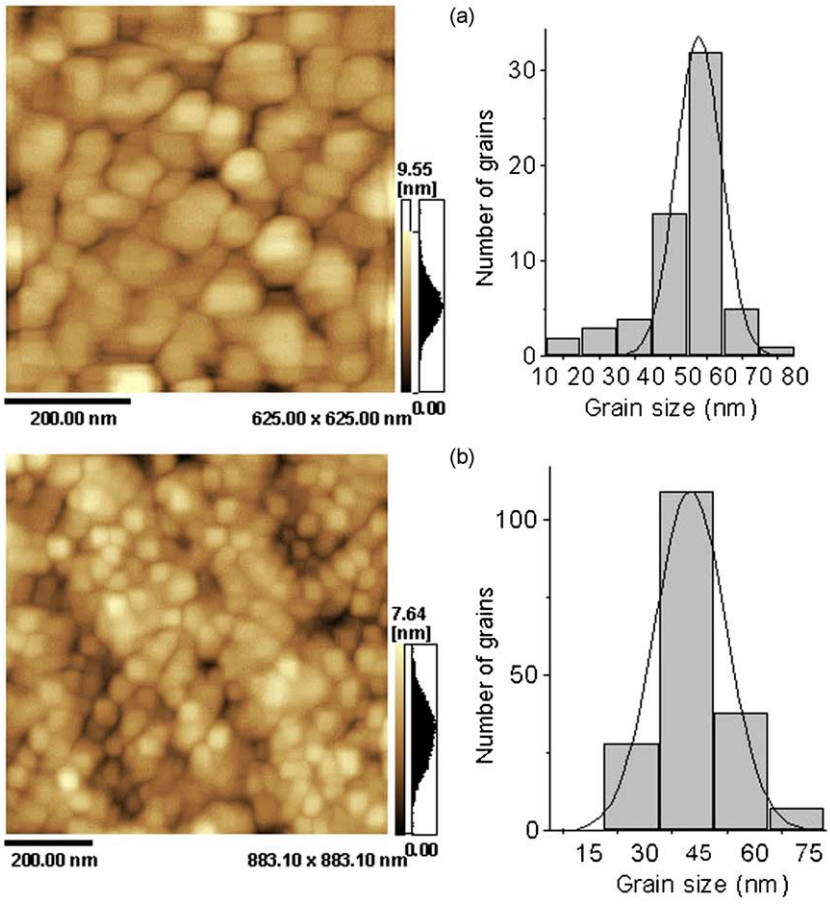

Fig. 6. Typical two dimensional AFM images of cobalt films deposited for (a) 1 and (b) 3 s alongwith the corresponding histograms showing grain size distribution.

the successive layers remained practically unaffected even for thicker multilayers.

3.4. X-ray investigation

Glancing angle XRD studies were employed to ascertain formation of coherent multilayers of Cu/Co using pulse deposition. The GAXRD data recorded for a sample with 40 bilayer period at a glancing angle of 1°, exhibited the main Braggs peaks corresponding to (111) and (200) reflection of copper substrate. Fig. 8 shows a typical experimental result recorded between $2\theta = 48–53°$. The pulse height employed for copper and cobalt deposition programmes were -0.35 and -1.1 V (vs SCE). The sharp reflex at $2\theta = 50.4°$

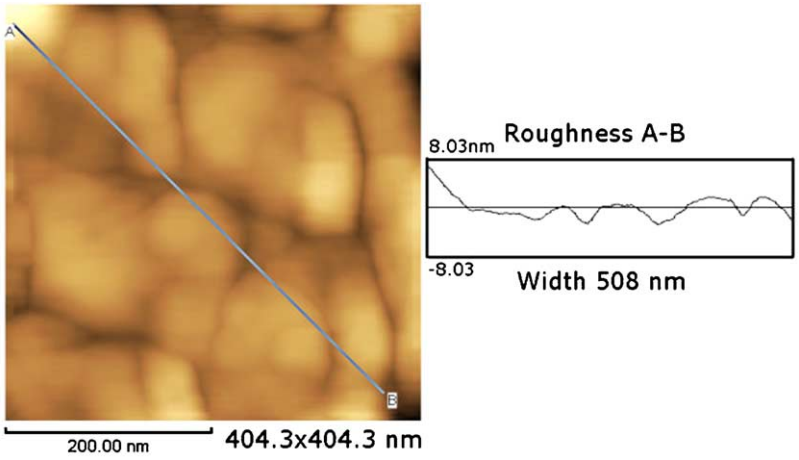

Fig. 7. Two dimensional AFM image and the roughness profile of top surface (Co) of Cu/Co(Cu) multilayer film with 40 bilayer periods.

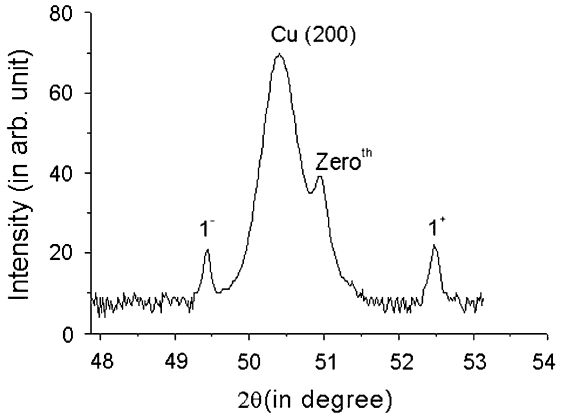

Fig. 8. Glancing angle X-ray diffraction data recorded for Cu/Co(Cu) multilayer film with 40 bilayer periods. The pulse height employed for copper and Cobalt deposition programmes were −0.35 and −1.1 V (vs SCE).

corresponds to main diffraction peak for (200) planes of the copper substrate. The zeroth order main diffraction peak of the Cu /Co(Cu) multilayer can be seen at 50.9° near (200) peak of Cu. This multilayer peak can be seen to be flanked by the first order satellite peaks marked as 1^+ and 1^- at $2\theta = 49.5°$ and 52.5°, respectively.

The presence of satellite peaks in Fig. 8 provides conclusive evidence of the existence of a multilayer structure with a bilayer periods (Λ) and lattice spacing (d) which are related by

$$\frac{2 \sin \theta_{\pm 1}}{\lambda} = \frac{1}{d} \pm \frac{n}{\Lambda} \quad (1)$$

were n is the order of the satellite peaks and λ (=1.54 Å) is the wavelength of X-rays. For Ist order satellite peaks ($n=1$) the average bilayer period calculated from Eq. (1) was found to be 6.2 nm.

Our observations therefore, provide evidence of growth of coherent multilayers.

4. Conclusion

The electrodeposition behavior of copper, cobalt and nickel have been studied using cyclic voltammetry. The possibility of deposition of oxide of cobalt and copper between −0.57 and 0.65 V has been revealed during the cathodic scan of the substrate potential. X-Ray diffraction studies of thin films electrodeposited at −0.65 V were used as additional supporting evidences, indicating formation of $CoCuO_2$. The cathodic onset for deposition of copper and cobalt have been shown to be widely separated and well resolved facilitating growth of Cu/Co multilayers. The evolution of surface morphologies following successive electrodeposition pulses were also studied using atomic force microscopy. It has been shown that the pulse deposition programme used in this study leads to reduction in the surface roughness. The average surface roughness of the electrodeposited Cu and Co layers were found to be 1.3 and 1.1 nm. The surface roughness did not change significantly even after deposition of 40 bilayers of the Cu/Co(Cu).

Glancing angle X-ray diffraction studies of the as grown Cu/Co(Cu) multilayers revealed sharp reflexes flanked by satellites. Formation of coherent multilayers using electrodeposition technique can thus be concluded.

Acknowledgements

This work was carried out from the research grants received from the Department of Science and Technology Govt. of India, New Delhi and the Special Assistance/COSIST program grant of UGC, New Delhi. These are gratefully acknowledged.

References

[1] M. Kaneko, J. Magn. Magn. Mater 148 (1995) 351.
[2] K.M.H. Lenssen, D.J. Adelerhof, H.J. Gassen, A.F. Kuiper, G.H.J. Somers, J.B.A.D. Van Zon, Sensors and Actuators 85 (2000) 1.
[3] L. Peter, A. Cziraki, L. Pogany, Z. Kupay, L. Bakonyi, M. Uhlemann, M. Herrich, B. Arnold, T. Bauer, K. Wetzig, J. Electrochem. Soc. 148 (2001) C168.
[4] P.C. Yashar, William, D. Sproul, Vacuum 55 (1999) 179.
[5] A.J.R. Ives, J.A.C. Bland, T. Thomson, P.C. Riedi, M.J. Walker, J. Xu, D. Greig, J. Magn. Magn. Mater. 154 (1996) 301.
[6] C. Spezzani, P. Torelli, M. Sacchi, R. Delaunay, C.F. Hague, V. Cros, F. Petroff, Appl. Phys. Lett. 81 (2002) 3425.
[7] C.M. Son, G. Lucadamo, K. Barmak, J. Appl. Phys. 80 (1996) 6689.
[8] J. Schuhrke, J. Zweck, H. Hoffmann, Thin Solid Films 292 (1997) 118.
[9] P.R. Aitchison, J.N. Chapman, D.B. Jardine, J.E. Evetts, J. Appl. Phys. 81 (1997) 3775.
[10] J.A. Borchers, P.M. Gehring, C.F. Majkrzak, A.M. Zeltser, N. Smith, J.F. Ankher, J. Appl. Phys. 81 (1997) 3771.
[11] J.S. Manoharan, J. Sheh, H. Jenniches, M. Klaua, J. Kirschner, J. Appl. Phys. 81 (1997) 3768.
[12] A. Blondel, B. Doudin, J.-Ph. Ansermet, J. Magn. Magn. Mater. 165 (1997) 34.
[13] L. Wang, K. Yu-Zhang, A. Metrot, P. Bonhomme, M. Troyon, Thin Solid Films 288 (1996) 86.
[14] G.R. Pattanaik, D.K. Pandya, S.C. Kashyap, J. Electrochem. Soc. 149 (2002) C363.
[15] H. Zaman, A. Yamada, H. Fukuda, Y. Ueda, J. Electrochem. Soc. 145 (1998) 565.
[16] T.A. Green, A.E. Russell, S. Roy, J. Electrochem. Soc. 145 (1998) 875.
[17] J.J. Kelly, P.E. Bradley, D. Landolt, J. Electrochem. Soc. 147 (2000) 2975.
[18] G. Nabiyouni, O.I. Kasyutich, S. Roy, W. Schwarzacher, J. Electrochem. Soc. 149 (2002) C218.
[19] M. Alper, P.S. Aplin, K. Attenborough, D.J. Dingley, R. Hart, S.J. Lane, D.S. Lashmore, W. Schwarzacher, J. Magn. Magn. Mater. 126 (1993) 8.
[20] J. Yahalom, O. Zadok, J. Mater. Sci. 22 (1987) 499.
[21] M. Shima, L.G. Salamanca-Riba, R.D. McMichael, T.P. Moffat, J. Electrochem. Soc. 148 (2001) C518.

[22] N. Zech, E.J. Podlaha, D. Landolt, J. Electrochem. Soc. 146 (1999) 2886.
[23] A. Brenner, Electrodeposition of Alloy, Acadmic Press, New York, 1963.
[24] M.E. Bahrololoom, D.R. Gabe, G.D. Wilcox, J. Electrochem. Soc. 150 (2003) C144.
[25] S.P. Jiang, A.C.C. Tseung, J. Electrochem. Soc. 137 (1990) 3381.
[26] D. Gupta, A.C. Nayak, J. Mazher, R. Sengar, K.P. Joshi, R.K. Pandey, J. Mater. Sci. 39 (2004) 1–6 (see also p. 1615).
[27] R.K. Pandey, S.N. Sahu, S. Chandra, In: Hand Book of Semiconductor Electrodeposition, Marcel Dekker Inc., New York, 1996. p. 107.